Construction and Building Materials 451 (2024) 138832

Contents lists available at ScienceDirect

Construction and Building Materials

journal homepage: www.elsevier.com/locate/conbuildmat

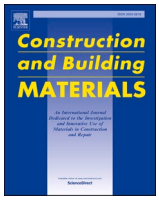

Natural thermal and hygrothermal regulation with heavy cob for low carbon construction

Aguerata Kabore [a], Aziz Laghdir [b], Claudiane Ouellet-Plamondon [a,*]

[a] Department of Construction Engineering, École de technologie supérieure, Université du Québec, 1100 Notre-Dame Street West, Canada
[b] Serv Rech & Expertise Transformat Prod Fore (SEREX), Cégep de Rimouski, Amqui, Quebec G5J 1K3, Canada

ARTICLE INFO

Keywords:
Hygrothermal properties
Moisture buffer value
Geosourced materials
Wood frame structure
Open porosity
Cob walls

ABSTRACT

Modern construction has a growing interest in geosourced materials for their low carbon footprint. This study aims to investigate the hygrothermal properties of two clay materials reinforced with wheat fibres using the traditional heavy cob technique for modern wood frame construction. The water absorption coefficients (α_{mat}), water vapor permeability (δ), water vapor diffusion resistance (μ), moisture diffusivity (D_W), moisture effusivity (b_m), equivalent moisture penetration depth ($dp_{1\ \%}$), specific moisture capacity (ζ), theoretical and experimental moisture buffer value (MBV_{exp} and MBV_{theo}), porosity (η) and sorption isotherms were studied as a function of the fibre content in the samples of fibre percentages of 0 %wt, 3 %wt, and 6 %wt. The thermal conductivity (λ), heat capacity (C_p), thermal diffusivity (D), and thermal effusivity (E) were evaluated as a function of the moisture content. The results indicate that the moisture buffering capacity of the clay samples, with and without fibre reinforcement, is greater than 2 g/(m^2. %RH). The open porosities of the samples varied from 20 % to 45 %, with specific moisture capacities from 0.014 to 0.031 kg/kg. The equivalent moisture penetration depth of the samples ranged from 2.17 cm to 2.68 cm. After the exposure of the cob wall containing 3 %wt fibre to temperatures of −5 ℃, 20 ℃, 35 ℃, and 45 ℃, the experimental results of the interior temperature of the wall varied between 19.5 ℃ and 23 ℃. It is therefore recommended to use cob containing at least 3 % or more fibre for wall construction in a real environment.

1. Introduction

Buildings and the construction sector account for nearly 40 % of CO_2 emissions related to energy and the material manufacturing process [1]. Buildings use various materials that consume energy and emit CO_2 throughout their life cycle, known as embodied energy and embodied carbon. With increasing urbanization, the number of residential buildings continues to rise, significantly impacting carbon emissions. Understanding the emissions from the construction sector [2] and the entire construction process, including extraction, manufacturing, transport, construction, and the building's life cycle, contributes to identifying measures to reduce CO_2 emissions [3]. Defining net-zero carbon and low carbon footprint construction also become crucial concepts to achieve global climate goals [3]. The International Energy Agency (IEA) highlights the importance of government commitments and technological innovations to reduce carbon emissions in the construction sector. Geo-sourced materials in modern building construction are becoming essential due to their low carbon footprint and recyclability [4–6].

Currently, clay stabilized with cement and with rammed earth represents modern traditional building techniques. The dynamic compaction of the mixture in temporary boxes is most employed commonly for production bricks or designing rammed earth walls. Its use is widespread in Australasia, Asia, Spain, Germany, France, and Great Britain [7,8]. Raw earth is an abundant building material with low grey energy; it is locally available, easy to work, and meets several environmental sustainability criteria. It has grown to become the most explored material for its integration into modern construction [9]. One of the main qualities of earth materials is their ability to regulate internal humidity thanks to their hygroscopic properties [10–15]. The main drawback is their vulnerability when in contact with water [16]. Indeed, the addition of plant fibres such as flax, hemp, or wheat can increase the resistance of earth materials to moisture and adverse weather conditions [17]. These plant fibres are ecological and biodegradable, and present numerous advantages, in addition to being recyclable, much like earth materials. Although various methods are used to make earth materials, the

* Corresponding author.
E-mail address: Claudiane.Ouellet-Plamondon@etsmtl.ca (C. Ouellet-Plamondon).

https://doi.org/10.1016/j.conbuildmat.2024.138832
Received 18 July 2024; Received in revised form 7 October 2024; Accepted 17 October 2024
Available online 29 October 2024

traditional technique of constructing with cob stands out for its simplicity and ecological character [18]. This technique generally involves mixing earth, plant fibres, and water to obtain a malleable material used to fill voids in timber-frame structure, commonly known as cob buildings [7]. The mixture must be plastic enough to adhere to the structure, but rigid enough to maintain its shape after drying [19].

Raw or stabilized earth containing a small quantity of cement can regulate the heat transfer but is not a very good insulator [20]. The stabilization of earth materials with cement limits their full recyclability at the end of their life [16,20], and affects their moisture retention capacity [21]. In agriculture, when wastes, also known as plant wastes, such as wheat fibre, rice fibre, corn fibre and cotton straw are present in large quantities, they pose a significant challenge because they can be potentially polluting to the environment [22]. These wastes are residues generated by the cultivation or raw processing of agricultural products. They can take the form of fibre or non-fibre materials and are available in abundant quantities almost throughout the globe [23]. Using plant fibres for reinforcement of earthen materials would improve the hydric properties of the latter while effectively removing the fibres from crop fields. Like raw earth, plant fibres are hygroscopic, renewable, and have a sustainable life cycle [9,24]. Earth reinforced with plant fibres produces little to no waste, has a very low or zero carbon footprint [25,26], and is part of hygroscopic composite materials [23]. The fibres are natural composites that are fully recyclable at the end of their life and their production requires local resources, little energy, and can be done at low cost. As these materials are hygroscopic, each element of a building designed with them is impacted by external moisture [27]. Managing the moisture of these elements is very energy intensive. To reduce the energy demand associated with this moisture management, these materials are increasingly being studied to improve their moisture properties. Poor moisture management can lead to fungal and mold growth in walls. If the moisture absorption/desorption of building materials is overestimated or underestimated, HVAC systems may need to be brought in to meet heating or cooling needs [28].

Africa is currently experiencing rapid population growth, which is in turn putting pressure on the housing stock, with demand being highest in the residential sector [29–31]. Many African countries are facing major housing-related challenges such as a lack of adequate infrastructure, slums, and high prices. There is currently a 51 million housing unit housing deficit on the African continent, and the number keeps increasing each year due to rapid population growth [32]. This housing crisis is particularly acute in countries such as South Africa and Djibouti, where rapid population growth and urbanization have created increased demand for affordable housing [33]. Authorities and stakeholders therefore have no choice but to implement effective housing policies promoting sustainable infrastructure development, while focusing on building affordable housing. Walls made of rammed earth with a wooden frame structure are soundproof, termite-resistant, and chemical-free, and the wooden frame provides good seismic resilience to the building structure [34,35].

To promote material in the construction sector, highlighting the results of laboratory tests evaluating its thermal and hydric performance is essential for proving its viability [36]. Assessing and quantifying the hygrothermal properties of cob allows for the preservation and enhancement of traditional construction techniques, while also facilitating the scientific documentation of its performance. This can position cob as a viable, ecological, and sustainable option for contemporary construction. Although several studies have explored the potential of the cob and discussed it in the works of Kamal Haddad [37], as well as some data on the thermal performance of 3D-printed cob [38], a comprehensive understanding of the formulation [39], its mechanical [40], and hygrothermal properties for cob formulated using the traditional technique for sustainable construction remains to be evaluated. Moreover, it is important to provide clear guidelines for preparing the cob mixture to facilitate the construction process of cob buildings and ensure their hypothermic performance [41]. A lack of information on all the hygrothermal properties of cob materials, formulated using the traditional cob production technique, has been observed. This lack is especially regarding the evolution of their behavior at 75 % humidity, the free saturation coefficient (water saturation in the free state), the hydric inertia coefficients (D_w and b_m), the penetration degree ($dp_{1\ \%}$), and the specific water capacity (ζ). These coefficients are essential for the hygrothermal simulation of wall systems in different climatic zones. Evaluating all hygrothermal properties of traditionally produced cob using advanced techniques leads to a better understanding of its behavior, providing objective data on its thermal and hygroscopic characteristics, thereby optimizing its overall performance while respecting traditional know-how. This approach can also contribute to beefing up the construction technique and paving the way to the reintegration of cob in construction, particularly in a bid to meet energy efficiency and thermal comfort criteria in housing.

This article presents an experimental study of the influence of moisture content on the thermal and hygroscopic properties of wheat fibre-reinforced clay specimens manufactured using the heavy cob technique. Cob, as a natural material, has several sustainable advantages over conventional building materials [42]. This article examines the thermal conductivity, heat capacity, thermal diffusivity, and thermal effusivity of cob under varying moisture content, as well as the hydric properties of fibre-free and fibre-reinforced clay mixtures. The thermal performance of a mini-wall was also evaluated based on climatic data from Djibouti and Johannesburg, two African cities. The novelty of this work lies in the meticulous experimental evaluation of the hygrothermal properties and thermal performance of heavy cob, a traditionally made material that is easily reproducible on construction sites. This study presents comprehensive data on the hygrothermal properties of this cob in order to deepen the understanding of its hygrothermal behavior as a function of moisture content and to optimize its performance for sustainable construction while respecting traditional know-how.

2. Materials and methods

2.1. Materials

For the fabrication of the test samples, two types of clay, red clay, and beige clay in powder ranging in size from 0 to 63 μm, and wheat fibres were used. Red (Redstone) and beige clays (Midstone) were from Plainsman (Alberta, Canada), and the wheat fibres were obtained from the Institut de Recherche et de Développement en Agroenvironnement (IRDA) in Quebec, Canada, respectively [4]. The red clay (RC) is a clay containing iron oxide with a plasticity index of 15 %, while beige clay (BC) contains more kaolinite with a plasticity index of 16 % [4]. The plasticity index was determined in accordance with Canadian standard CAN/BNQ-2501–090 [43], and details of this work are available in Kabore and Ouellet-Plamondon [5]. Both clays contain 43 % quartz, 8.9 % kaolinite, and 2.2 % hematite for the red clay, and 25.8 % kaolinite and 0.1 % hematite for the beige clay [40]. The mineralogical composition was determined by X-ray diffraction (XRD), chemical analysis by X-ray fluorescence (XRF), and thermogravimetric analysis (TGA) using the Perkin Elmer STA8000 instrument, and the description of the methods is available in [40]. The particle size distribution and methylene blue value are available elsewhere [44]. For the tests in this study, three mixtures, with 0 %wt, 3 %wt, and 6 %wt fibre content, were prepared, with three replicates for each mixture, for every clay type, and for each test. The results for each property presented in this article are therefore the averages of three repetitions for each mixture. The fibre-free red and beige clay samples studied were made with a 25 % wt water/clay ratio. For the samples reinforced with 3 %wt and 6 %wt fibre, the fibres were first wetted with a water quantity corresponding to a water/fibre ratio of 205 %wt ± 15 %wt. This value was obtained from the water absorption test conducted on the fibres. The clay/water mixture was then made with 25 %wt water before the moistened fibres were added.

The samples were produced using the traditional cob production method, which uses raw fibres without chemical treatment. These fibres had a length ranging from 0.4 cm to 40 cm. The mixing process was done manually, beginning with blending clay and water until a consistent mixture was achieved. Subsequently, fibres were added to finalize the mix. A one-hour break was taken after the clay-water-fibre mixture was prepared to allow the entire mixture to reach moisture equilibrium before the samples were fabricated. A 254 × 254 × 25 mm^3 rectangular formwork and a 30 mm height and 36 mm diameter cylindrical formwork were used, depending on the type of test being conducted (Fig. 1). The formwork was filled and pressed by the hand, but without measuring the degree of compaction. This technique is commonly used for wood-frame structures. The specimens were dried in an oven set at 30 ℃ for 10–11 hours after demolding to ensure maximum water removal before their exposure to 23 ℃ ambient laboratory air. More information can be found in the previous article [4].

2.2. Methods

2.2.1. Determination of water content and water absorption/desorption of fibres

Before the tests were started, the initial moisture content of the fibres was determined. The fibres were taken directly from the bags and dried in an oven at 50 ℃ for 2 hours. The moisture was first calculated for a drying time of 2 hours. Subsequently, the fibres were returned to the oven at the same temperature for 1 hour to verify that they were completely dry before determining the initial moisture content. The moisture content obtained between these two drying intervals was 0 %. The moisture content of the fibres was calculated using Eq. 1 [45].

$$w_i = \frac{m_{wet} - m_{dry}}{m_{dry}} * 100\% \quad (1)$$

where w_i is the initial water content in %, m_{wet} is the mass of the sample before drying (fibre taken directly from the bag) in grams (g), and m_{dry} is the mass of the sample after drying in grams (g).

For the water absorption and desorption test, the wheat fibres were cleaned with distilled water and dried in an oven at 50 ℃ for 4 hours before testing. The fibres were then separated into three 5-gram samples for the water absorption test, according to the ASTM D2654 guidelines [46] referenced in a previous study, to determine the water absorption of the flax and hemp fibres [47]. Each sample was completely immersed in distilled water at different temperatures (23, 40, and 50 ℃). Some tests were performed at room temperature (23 ℃). For the tests conducted at 40 ℃ and 50 ℃, each sample was submerged in distilled water, and then placed in an oven set to the respective temperature. The containers were closed to prevent surface drying of the fibres. The weight of wet fibres was measured at regular intervals until saturation of the fibres (constant mass). To assess a fibre's ability to release absorbed moisture during testing, all samples were exposed to ambient laboratory air at a temperature of 23 ℃ and relative humidity ranging from 40 % to 50 % after the water absorption test, following saturation. The samples were weighed every 2 hours until completely dry (back to the initial mass before the water absorption test). Water content absorbed or lost at time t is calculated by applying Eq. 1.

2.2.2. Density and open porosity measurements

The open porosity of the samples was determined by combining the gas pycnometer method using helium and the non-wetting oil immersing method (olive oil). The open porosity of a porous material refers to the proportion of voids in the material that are interconnected and accessible from the outer surface. The oil test method was performed by NF ISO 5017 [48]. The gas pycnometer used for the measurement of the solid density and solid volume of the samples is an effective tool for determining the true density and the true volume (density and volume of the material without pores) of porous materials. The apparent density of a porous material is the density of the solid material, including the pores it contains. The true or solid density of a porous material, on the other hand, is the density of the solid portion of the material. In this study, a ULTrapyc 5000 gas pycnometer was used to determine the true density and the true volume of clay without fibres and with 3 %wt and 6 %wt fibre. The instrument was calibrated at a helium pressure of 20 psi and a temperature of 23 °C. Three samples 30 mm in height and 36 mm in diameter were made with the same mixture, for a total of nine samples. Before the solid and void volumes were measured, the samples were dried in an oven at 60 °C for 24 hours. To determine the void volume, the dried samples were first saturated with non-wetting oil under vacuum in a desiccator for 24 hours at a pressure of 80 kPa. This allowed the oil to replace the air in the open pores without interacting with the samples. Fig. 2 illustrates the steps for determining the open porosity of the samples.

The volume of the oil-filled voids was determined by the ratio of the mass of the oil to the density of the oil. Eq. 2 was used to determine the open porosity:

$$\eta = \frac{V_{voids}}{V_{voids} + V_{true}} * 100\% \quad (2)$$

where η is the porosity open (%), V_{voids} are the void volumes (m^3) and V_{true} is the true volume, I.e., the volume of the material without pores (m^3).

2.2.3. Thermal properties

The thermal properties of three different mixtures (0 %wt, 3 %wt, and 6 %wt fibre content) were initially measured in a dry state, with three replications for each mixture. For this, samples were dried in an oven at 105 ℃ for 48 hours. Two weighing were performed at 24 hours intervals, and a mass difference of less than 0.01 % was observed before

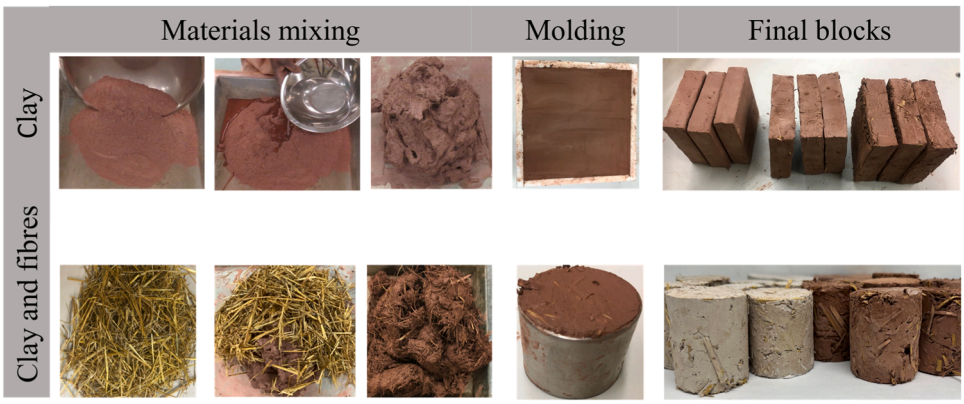

Fig. 1. Sample preparation protocol of earth and cob blocks developed.

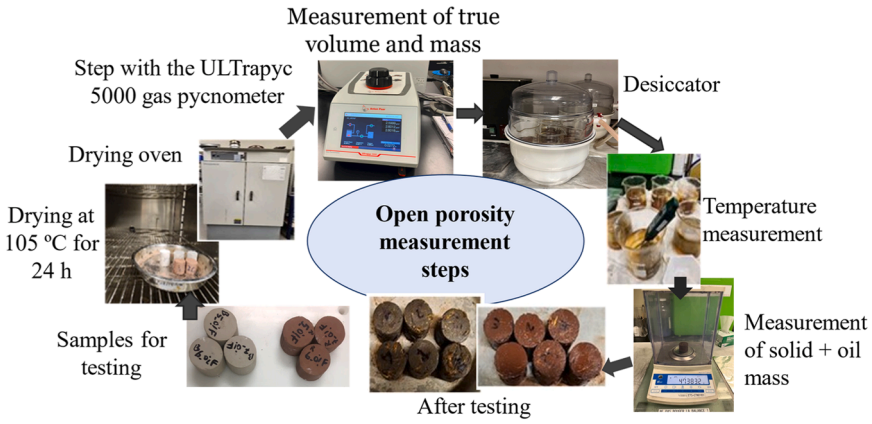

Fig. 2. Open porosity measurement.

testing. The tests were performed sample by sample to avoid moisture recovery with an MTPS (transient plane source modified) instrument according to the ASTM D7984 standard [49]. Further tests were performed on samples conditioned at ambient laboratory temperature and relative humidity (23 °C and 50 % RH), and with a sodium chloride (NaCl) solution, giving a relative humidity of 75 % RH at a 23 °C temperature. The water content that was either absorbed by the samples was measured before the tests. These measurements were aimed at observing the influence of moisture on the thermal properties of fibre-reinforced clay materials.

2.2.4. Water absorption test

Two methods were used to evaluate the water absorption capacity or relative humidity of the materials manufactured for this study, in accordance with ISO 15148 [50].

- Capillary absorption method (partial immersion): this test consisted of partially immersing the samples in a jar containing water for 24 hours. The change in the mass of each sample was determined by weighing it at given time intervals, and the water absorption was determined by Eq. 3.
- Moisture absorption method: a salt solution was prepared with sodium chloride (NaCl) to obtain a saturated solution, enabling maintaining the relative humidity at 75 ± 0.4 %, and the temperature at 23 ± 1 °C during the tests. The samples were then dried at 105 °C in an oven for 48 hours. The first weighing was done at the 24-hour drying mark, and a second weighing was carried out 24 hours after the first one. The difference in mass between the two weighing was 0.01 %. The samples were then placed in a sealed container with a tray containing the saturated sodium chloride (NaCl) solution and conditioned for 48 hours before the water content absorbed by the samples was measured.

$$\alpha_{mat} = \frac{m_{wet} - m_{dry}}{m_{dry}} * 100\% \quad (3)$$

where α_{mat} is the water absorption coefficient in %, m_{dry} is the mass of the sample in a dry state in g, and m_{wet} is the mass of the sample in a wet state in g.

2.2.5. Water vapor permeability and resistance factor

The measurement of water vapor permeability was determined by the wet and dry cup methods according to the ASTME96 standard [51].

- Dry cup: the samples were sealed in a cup containing a desiccant (silica gel) that maintained the relative humidity of the atmosphere in the cup at 0 % RH, leaving a small air space between the desiccant and the samples (Fig. 2a).
- Wet cup: the samples were sealed in a cup containing distilled water that maintained the relative humidity of the atmosphere in the cup at 100 %RH, leaving a small air space between the distilled water and the samples (Fig. 2b).

The test chamber was maintained at a constant temperature of 23 °C ± 1 °C and a relative humidity of 50 % RH ± 2 % RH. The sample and the cup assembly were then placed in an apparatus equipped with a balance for periodic sample mass measurements that determined the rate of water vapor movement through the sample into the desiccant or to the controlled chamber atmosphere. Fig. 3 shows the samples' water vapor permeability measurement principle.

At equilibrium, the water vapor permeability (δ) was then determined by Eq. 4 and the water vapor diffusion resistance (μ) by Eq. 5:

$$\delta = \frac{G * e}{\Delta Pv} \quad (4)$$

$$\mu = \frac{\delta_a}{\delta} \quad (5)$$

where ΔPv is the water vapor pressure difference in Pa [10] (Eq. 6):

$$\Delta Pv = (HR_1 - HR_2) * 610.5 * e^{\left(\frac{17{,}269*T}{237{,}3+T}\right)} \quad (6)$$

where e is the thickness of the sample in m, G is the water vapor transmission rate

$G = \frac{\Delta m/\Delta t}{S}$ in kg/(m^{2}s) [51], S is the average surface area of the exposed sample in m^2, Δm is the weight change in kg, Δt is the time interval during which water vapor transmission occurred in s, δ_a is the water vapor permeability of water (2.10^{-10} kg/(m^2.s. Pa)), and T is the temperature in K.

2.2.6. Moisture buffer value

Moisture buffer values (MBV) were measured using the NORDtest protocol [52]. Measurements were made on 254 × 254 × 25 mm^3 (10-inch x 10-inch x 1-inch) samples. Prior to testing, the samples were

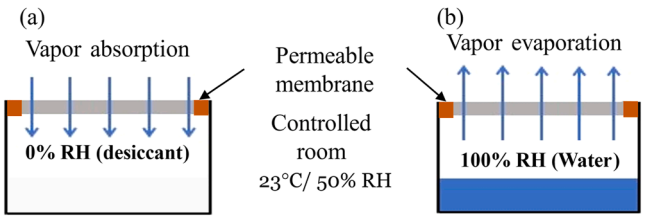

Fig. 3. Water vapor permeability measurement principle: a) dry cup and b) wet cup.

sealed on all sides with aluminum tape except for one side and then conditioned at 23 ℃ ± 5 ℃ and 50 % RH ± 5 % RH. After moisture equilibrium, the test samples were placed in a climate chamber and exposed to several cycles of relative humidity (8 h at 75 % RH and 16 h at 33 % RH). The equilibrium criterion was a period long enough for the mass of the samples to stabilize such that the difference between two successive determinations (24 hours apart) of the mass was within 0.01 %. The MBV of the samples at each cycle was calculated by Eq. 7:

$$MBV = \frac{\Delta m}{A(75\%RH - 33\%RH)} \quad (7)$$

where MBV is the moisture buffer value in g/(m^2. %RH), Δm is the mass variation (water sorption/desorption) of the samples during the period of high or low relative humidity in g, and A is the surface of the sample m^2.

2.2.7. Sorption, desorption isotherm curves, and specific moisture capacity

The Dynamic Vapor Sorption (DVS) method based on the ISO 12571 standard [53] was used for the tests (Figure S1). Samples (three per mix) of 0 %wt, 3 %wt, and 6 %wt fibre, 62 mm in diameter and 23 mm thick, were placed in a climate chamber on one side of a microbalance (DVS2 from SMS Ltd., UK). The relative humidity of the climate chamber varied in successive steps from 20 % to 95 % RH in 15 % RH increments. The microbalance device controlled the temperature (set at 23 ± 0.5 ℃) and humidity around the sample placed in a basket suspended from the weighing system. The mass of the samples was measured at regular intervals. Moisture equilibrium was reached when the mass variation did not exceed 0.0005 % for each moisture level.

The specific moisture capacity (ξ), which represents the slope of the moisture retention curve between 35 % and 75 % RH, assumed to be linear, was determined by Eq. 8 from the experimental sorption data. The moisture effusivity (b_m) and moisture diffusivity (D_w), which are used to evaluate the moisture transport in building materials under a saturating vapor pressure gradient, were calculated by Eqs. 9 and 10 using the vapor permeability value obtained by the wet cup method [52]:

$$\xi = \frac{dw}{dRH} \quad (8)$$

$$b_m = \sqrt{\frac{\delta.\rho_0.\xi}{Pvs}} \quad (9)$$

$$D_w = \frac{\delta.Pvs}{\rho_0 \xi} \quad (10)$$

where dw is the difference in water content, dRH is the difference in relative humidity, δ is the water vapor permeability determined by the wet cup method, ρ_0 is the dry density, Pvs is the saturation vapor pressure, depending on the test conditions and calculated by Eq. 11, and Pa is the atmospheric pressure:

$$Pvs = Pae^{\left(13.7 - \frac{5120}{T(23°C)}\right)} \quad (11)$$

The theoretical moisture buffer value (MBV_{theor}) and the equivalent moisture penetration depth ($dp_{1\%}$) in a porous material were calculated by Eqs. 12 and 13. These coefficients are simplified approaches used to evaluate the moisture variation capacity of building materials [52]:

$$MBV_{Theor} = 0.00568.Pvs.bm\sqrt{tp} \quad (12)$$

$$dp1\% = 4.61\sqrt{\frac{Dw.tp}{\pi}} \quad (13)$$

where Pvs is the saturation vapor pressure, b_m is the moisture effusivity, tp (s) is the period corresponding to 24 hours, D_w is the moisture diffusivity.

2.2.8. Statistical test

The data presented in this article are shown as means ± standard deviation (SD) of three or more independent replicates. All results presented in tables and figures were subjected to a one-factor ANOVA for groups of more than three or to a paired samples t-test. The t-test is a statistical method used to compare paired means in a specific manner. Individual means were compared to identify significant differences with a α-value of 0.05, and a significant difference is observed for p less than the α-value ($p < 0.05$).

2.2.9. Indoor temperature and humidity in cob on a wall element

Measurements of temperature variations through the mini-walls were conducted on 80 cm width, 80 cm length, and 15 cm thickness walls. Before testing began, the walls were preconditioned at a temperature of 20 °C and a relative humidity of 50 % in a climate chamber. Testing began once the temperatures and humidity of the mini-walls had stabilized. The biclimatic chamber used for experimental thermal performance testing is an EXCAL 7713-HA + 7723-HA model from the manufacturer CLIMATS, and it consists of two chambers, one for simulating indoor conditions in terms of temperature, and the other for outdoor conditions. The operating principle of the biclimatic chamber is to monitor the thermal behavior of a wall sandwiched between the two chambers using a sample holder. Temperature sensors are placed at various positions within the wall thickness (on the interior surface, exterior surface, and in the middle), allowing the characterization of the wall's thermal performance. The testing and sensor placement procedure is identical to the procedures described in the work of Sawadogo et al. [54] using the same equipment. The two cities studied, Djibouti with temperatures ranging from 20 °C to 45 °C, and Johannesburg with temperatures between −5 °C and 35 °C were chosen due to the suitable temperature range of these two cities. City information was obtained by purchasing climate data from the Weather API [55]. Djibouti has higher temperatures, with a maximum of 45 °C, while Johannesburg has lower temperatures, reaching −5 °C. To start the measurements, the outdoor temperature was set at 20 °C and −5 °C for the winter session and 45 °C and 35 °C for the summer session, for Djibouti and Johannesburg respectively. Inside the enclosure, the temperature was maintained at 20 °C. This experimental measurement procedure was used to validate the results obtained from numerical data by Sawadogo et al. [54]. The purpose of this measurement in this study is to evaluate the capacity of the cob wall with 3 %wt fibres to transfer heat or lose heat from the interior side of the wall when the external temperature is high or low. Table 1 illustrates the outdoor and indoor conditions defined for the temperature and relative humidity measurements of the outside, middle, and inside walls, and Figure S2 in the supplementary document shows the equipment and the experimental wall. The measurements were conducted during seven consecutive days.

3. Results and discussions

3.1. Water absorption and desorption of fibres

Fig. 4 shows the evolution of the water absorbed by the fibres for 60 hours at different temperatures. The results of the water absorption test show that 25 minutes after being put in water, the fibres absorb about 205 ± 15 % of water compared to their initial mass, and the water absorption continues until saturation (60 hours) at room temperature (23 ℃). When the ambient temperature increases, the amount of moisture absorbed by plant fibres also increases. The temperature significantly influences the water absorption rate, with higher temperatures promoting water diffusion within the fibres. This can be explained by the fact that wheat fibres have very high capillary forces, which are impacted by the geometry of the fibres' pores [56]. Alfa fibres absorbed between 156 % and 640 % of their mass in water after

Table 1
Boundary conditions for experimental measurements on the wall element.

Cities	Outside wall				Inside wall	
	Winter		Summer		Winter and summer	
	Temperature (°C)	Relative humidity (%)	Temperature (°C)	Relative humidity (%)	Temperature (°C)	Relative humidity (%)
Djibouti	20 ± 1	90 ± 2	45 ± 1	30 ± 2	20 ± 1	50 ± 2
Johannesburg	−5 ± 1	90 ± 2	35 ± 1	25 ± 2		

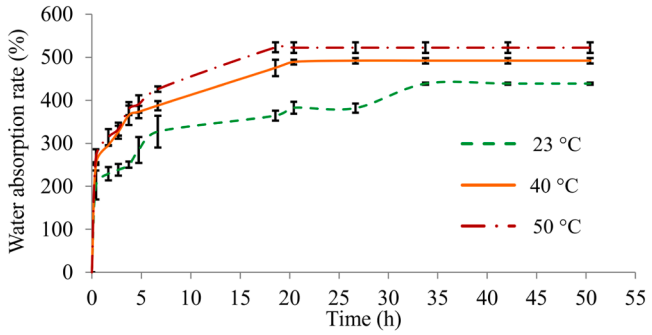

Fig. 4. Evolution of water absorption rate of wheat fibres as a function of immersion time and temperature.

saturation [57]. A recent study has demonstrated that pineapple fibres can absorb 268 % of their dry mass in water when immersed in water for one hour [58]. Other studies have also shown water absorption values ranging from 63 % to 300 % for different plant fibres [58,59]. The high water absorption of plant fibres is explained by their porous structure and the presence of hemicelluloses [57]. The drying times of fibres were evaluated in the present study and the results are presented in Figure S3 in the supplementary document. The complete saturation of the fibres took about 48 hours, while the drying time was 20 hours for all samples exposed to ambient laboratory air, a temperature of 23 °C, and a relative humidity ranging from 40 % to 50 % RH. The complete loss of water in the wheat fibre structure was relatively fast. This property allows the composite materials (fibre-reinforced clays) to keep the building elements (wood framing) durable and to prevent moisture from building up in the wall for several days during heavy rainfall. Figure S3 shows the evolution of mass loss of wheat fibres during drying.

3.2. True density and open porosity measurements

Fig. 5 presents the results of the samples' bulk density and true density measurements. The bulk density decreases significantly with increasing fibre content in the mixtures as compared to the solid density determined by the gas pycnometer. The fibre-free red and beige clay samples studied had a dry bulk density from 2016 ± 17 kg/m^3 to 1956 ± 16 kg/m^3. The average dry bulk density of the samples with 3 %wt fibre varied between 1662 ± 41 kg/m^3 and 1588 ± 39 kg/m^3, while for the samples with 6 %wt fibres, it varied between 1454 ± 66 kg/m^3 and 1315 ± 54 kg/m^3. The average density of the solid material was 2738 kg/m^3 to 2555 kg/m^3 for the red clay samples and from 2671 kg/m^3 to 2489 kg/m^3 for the beige clay samples. This represents a 7 % decrease in density for a 6 %wt fibre content in the solid matter for both types of clay. This observation is supported by previous research [9,60,61]. The significant difference observed between the average bulk density and the average solid density is presented in Fig. 4 by Δ(density). This difference in density becomes more significant for samples containing 3 %wt and 6 %wt fibre. As more fibres are added, Δ(density) increases. This can be explained by the increase of voids in the material due to the presence of fibres.

Fig. 6 presents the trends between the accessible porosity and bulk density of the samples. The bulk density decreases with the open porosity (correlation coefficient 0.99 for the red clay and 0.999 for the

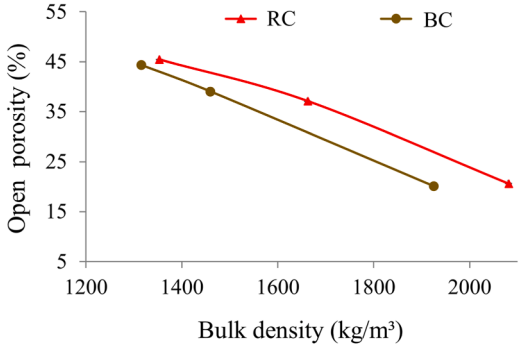

Fig. 6. Open porosity variation versus bulk density.

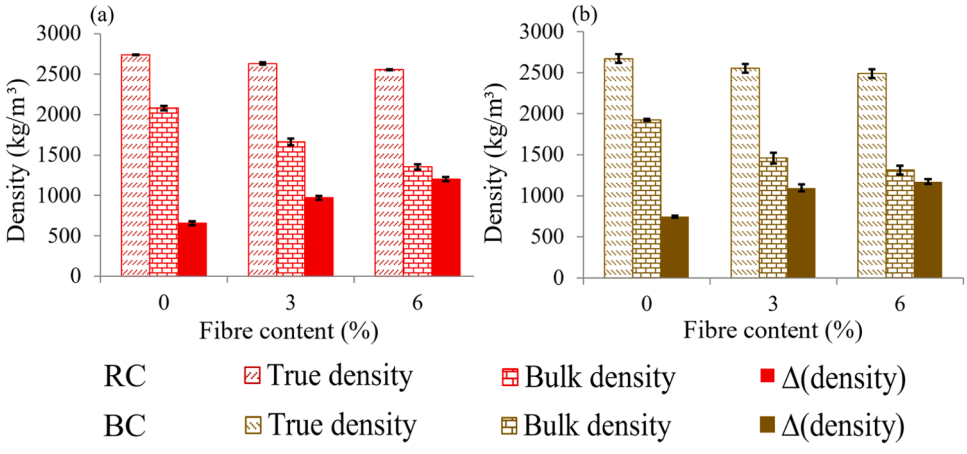

Fig. 5. True and apparent density of the (a) red and (b) beige clay samples.

beige clay). The average accessible porosity results are 20.6 % and 20.1 % for the red and beige clay samples without fibres, respectively. For the fibre-reinforced samples, a significant increase in porosity as a function of the bulk density of the samples was observed. The values obtained for the two types of clay of the same mixture are close, 37.1 % and 39.1 % for the red and beige samples reinforced with 3 %wt fibre, respectively. The porosity of red and beige clay samples reinforced with 6 %wt fibre was found to be 45.4 % and 44.4 %, respectively. A decrease in porosity followed by an increase in density can be explained by the fact that the clay particles feed the pores of the mixture, thus reducing the quantity of open pores in the materials without fibre reinforcement [62]. Porosity values ranging from 21.7 % and 41.6 % of compressed earth bricks, correlating with a density ranging from 2194 kg/m^3 and 1607 kg/m^3, respectively, were reported in [63]. Similarly, porosity values between 38 % and 44 % were documented for clay materials reinforced with olive pruning waste, with the density ranging from 1669 kg/m^3 to 1409 kg/m^3 [60]. Other research has also shown that porosity in clay materials increases with a higher proportion of fibres or plant aggregates, consequently affecting the bulk density of these materials [64,65].

The integration of fibres into earth materials increases porosity by reducing the compaction pressure, which decreases density and the contact between clay particles. Fibres act as spacers, creating larger voids and enhancing open porosity. They also form bridges between particles, strengthening the structure and preventing pore collapse. These structural modifications increase open porosity while reducing the bulk density of the samples. The high correlation coefficients confirm a strong relationship between density and open porosity, directly linked to the fibre content in the samples.

3.3. Influence of relative humidity on thermal properties

To evaluate the influence of moisture content on the thermal properties of clay and cob materials, all dry clay and cob samples were subjected to a relative humidity of 50 % RH and 75 % RH at 20 °C for 48 hours. The results of the measured water content are presented in Table 2 and represent the average of three samples per mixture. Figs. 7 and 8 illustrate the variation of thermal property values as a function of water content obtained from measurements performed with the modified transient plane source method according to ASTM D7984 [49]. The water content has a great impact on the thermal properties of the samples. Samples made with a 6 %wt fibres content tend to absorb more moisture than samples with 3 %wt and 0 %wt fibre content. This ability to absorb more water vapor may be attributed to the increased pore size caused by the presence of fibres in the clay matrix [66]. A 3.8 % water absorption led to an increase in thermal conductivity three times higher than the thermal conductivity obtained in the dry state for samples with 6 %wt fibre. The thermal conductivity of the other mixtures varied between 0.75 and 1.18 W/(m.K) and between 0.52 and 0.72 W/(m.K) for a water content from 3.1 % to 3.6 % for the mixtures without fibre and with 3 %wt fibre, respectively. These findings align with previous studies [65,67,68]. Additionally, research on earth samples with varying fibre content has shown that the thermal conductivity changes in relation to the amount of water absorbed by samples. This effect of water content on thermal conductivity was noted in studies involving clay samples with different sand compositions, as well as hemp and pith samples [69,70].

Table 2
Water content absorbed for a 48 hours exposure at 50 % RH and 75 % RH.

	Reference	Test condition and absorbed water content (%)	
	Fibre (%wt)	50 % HR and 23 °C	75 % HR and 23 °C
RC	0	1.19 ± 0.08	3.09 ± 0.08
	3	1.26 ± 0.08	3.58 ± 0.04
BC	6	1.31 ± 0.01	3.78 ± 0.07
	0	0.91 ± 0.01	2.24 ± 0.02
	3	1.00 ± 0.08	2.30 ± 0.07
	6	1.24 ± 0.10	2.69 ± 0.03

The specific heat of the fibre-free and fibre-reinforced red clay samples increased significantly with increasing water content, in contrast to the beige clay samples reinforced with 3 %wt and 6 %wt fibre. For the red clay samples, an increase of 11 % was observed for mixtures without fibre, 5 % for mixtures with 3 %wt fibre, and 9 % for mixtures with 6 %wt fibre. The beige clay samples reinforced with 3 % wt fibre showed a gradual decrease in their specific heat by 9 %, followed by an increase. In contrast, those reinforced with 6 %wt fibre initially exhibited a slight decrease in their specific heat of about by 2 %, before increasing by 8 %. The results obtained on the coefficients of thermal inertia (thermal diffusivity and effusivity) show that the values of the two coefficients increase with an increase in the water content of the material (Fig. 8). These values are higher than the values obtained on dry samples in previous studies [10,71]. The values of all the thermal properties mentioned in this article increase globally with the water content, but in different ways for each type of mix, and depending on the quantity of fibres present in the mix. This is due to the presence of fibres in the samples creating larger voids in their structure. In high humidity conditions, the air within the sample voids is replaced by water vapor, increasing the thermal properties of these materials. The higher the fibre content in the material, the greater its tendency to absorb water vapor (Table 2).

The absorption of water by clay and cob samples leads to an increase in their thermal conductivity, which reduces their effectiveness as insulators by facilitating heat transfer through the material. Moreover, the increase in water content also affects the specific heat capacity of the samples. In the case of red clay samples, this specific heat capacity increases significantly, suggesting a better heat storage capacity. However, this can also lead to a slower response to temperature variations, impacting thermal regulation [72]. Furthermore, the increase in thermal diffusivity and effusivity in the presence of moisture indicates that cob can adapt more quickly to temperature changes. The presence of fibres in the material's structure increases pore size, promoting greater absorption of water vapor. This characteristic can enhance the material's ability to regulate indoor humidity, but it comes at the expense of its insulating efficiency under high humidity conditions [62].

3.4. Hydric properties of samples

To assess the water performance of the cob, red or beige clay mixes with 3 %wt and 6 %wt fibre were used with a control mix without fibres. Their water vapor permeability, water vapor resistance factor, moisture buffer value (MBV) and sorption/desorption curve were evaluated.

3.4.1. Water absorption

Earthen building materials are sensitive to water. However, contact between water and the building envelope is often unavoidable. Laboratory tests to assess the degree of vulnerability are performed either by immersion or by capillary action. In the present work, the results of a capillary test and at 75 %RH exposure tests are presented. Fig. 9 shows the curves representing the variation of the capillary water absorption coefficient and moisture absorption obtained as a function of the fibre content in the samples. The coefficient of capillary water absorption and moisture absorption increases with increasing fibre content. The increase in water and moisture absorption of the fibre-reinforced samples can be explained by the hydrophilic nature of wheat fibres, which can absorb more water. Raw plant fibre-reinforced earth materials absorb more water when exposed to moisture than materials without fibre [73,74]. Capillary absorption tests conducted on samples reinforced with date palm fibres stabilized with 5–8 % cement have shown that the water absorption coefficient increased with an increase in fibre content in the material [23]. The same was observed for samples exposed at 75 %RH in this study.

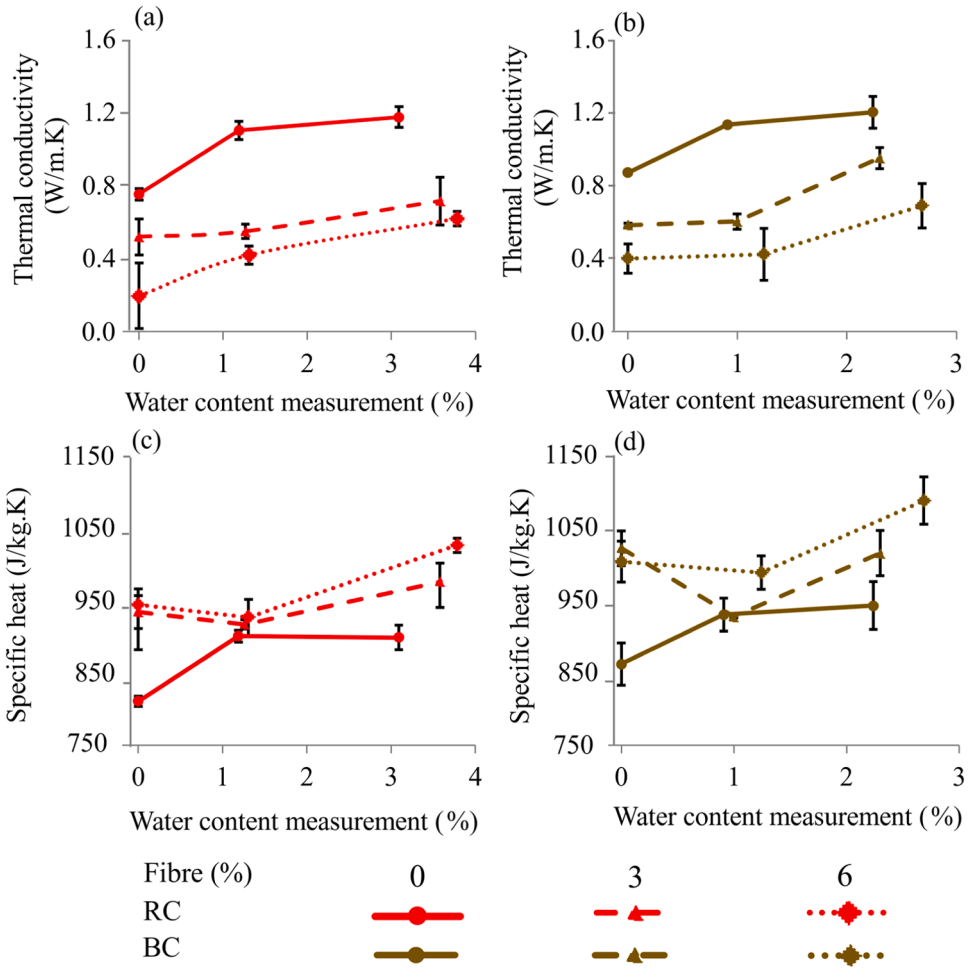

Fig. 7. Variation of thermal conductivity and specific heat with water content of (a, c) red clay samples and (b, d) beige clay samples.

3.4.2. Water vapor permeability and resistance factor

Table 3 and Fig. 10 show the mean values and standard deviations of the water vapor permeability and water vapor resistance factor of clay samples without and with fibre. The test results indicate that the water vapor permeability and the water vapor resistance factor depend mainly on the nature of the clays. The t-tests comparing the means of the data confirmed that the differences are significant ($n = 9$, $\alpha = 0.05$, p-value = 0.03 and 0.002 (dry method) and p-value = 0.003 and 0.02 (wet method), Table S2, supplementary information). The studied samples have a water vapor permeability that allows them to be a natural moisture regulator. These properties are therefore very beneficial for the wood/cob construction. The water vapor permeability (δ) and vapor diffusion resistance factor values of the clay samples are comparable to data on earth bricks obtained by other authors [10,75]. The results of water vapor permeability and water vapor resistance factor obtained by the dry cup method do not show a significant influence of adding plant fibres in the production of cob for all samples ($n = 6$, $\alpha = 0.05$, p-value = 0.5, Table S3, for supplementary information). However, with the wet cup, this difference is visible. According to some authors, the transfer of liquid in smaller pores has a major impact on the macroscopic transport of water in materials [76–78]. Water can be retained in small pores by capillarity, thus leading to an increase in water movement resistance through the materials. Our samples, being made using the traditional technique of cob production, can result in the creation of larger pores after drying due to the presence of fibres (fibre/clay matrix interfaces). This can explain the decrease in water permeability of the samples reinforced with fibres in our study, thus increasing resistance to vapor. The results from this study for fibre-reinforced clay samples are consistent with those reported by previous research, where samples reinforced with 3 %wt and 6 %wt barley straw also showed similar values [10]. The addition of fibre leads to an increase in the water vapor diffusion resistance factor [9,10]. However, other authors have obtained water vapor permeability values that increase with the fibres increase [79]. Therefore, the μ and δ values of composite materials are dependent on the type of fibres used in their fabrication and the method of fabrication of the composite materials.

3.4.3. Moisture buffer value

Fig. 11 shows the average moisture buffer value (MBV) of each mixture with and without fibres. The experimental moisture buffer values (MBV_{exp}) of the samples are excellent. The MBV of the red clay samples without and with 3 %wt fibre is higher than that of the beige clay. On the other hand, with 6 %wt fibre in the mix, the MBV values of the beige clay samples are higher than those of the red clay. The samples formulated without fibre reinforcement have higher moisture buffer values than those reinforced with 3 %wt and 6 %wt fibre. The MBV values of all samples obtained after the tests are excellent according to the NORD test criterion (value greater than 2 g/(m^2.%RH)) [52]. The average results are 6.04 g/(m^2. %RH) and 4.22 g/(m^2. %RH) for the 0 % wt fibre samples (red and beige clay, respectively), 5.53 g/(m^2. %RH) and 2.78 g/(m^2. %RH) for the 3 %wt fibre samples and 3.19 g/(m^2. % RH) and 4 g/(m^2. %RH) for the 6 %wt fibre samples, respectively.

The effect of fibres on MBV in earthen materials reinforced with 3 % wt and 6 %wt barley straw was studied by Laborel-Préneron et al. [10], and a 21 % decrease in MBV was observed with the addition of 6 %wt barley straw. In the present study, adding 6 %wt wheat fibre to red clay

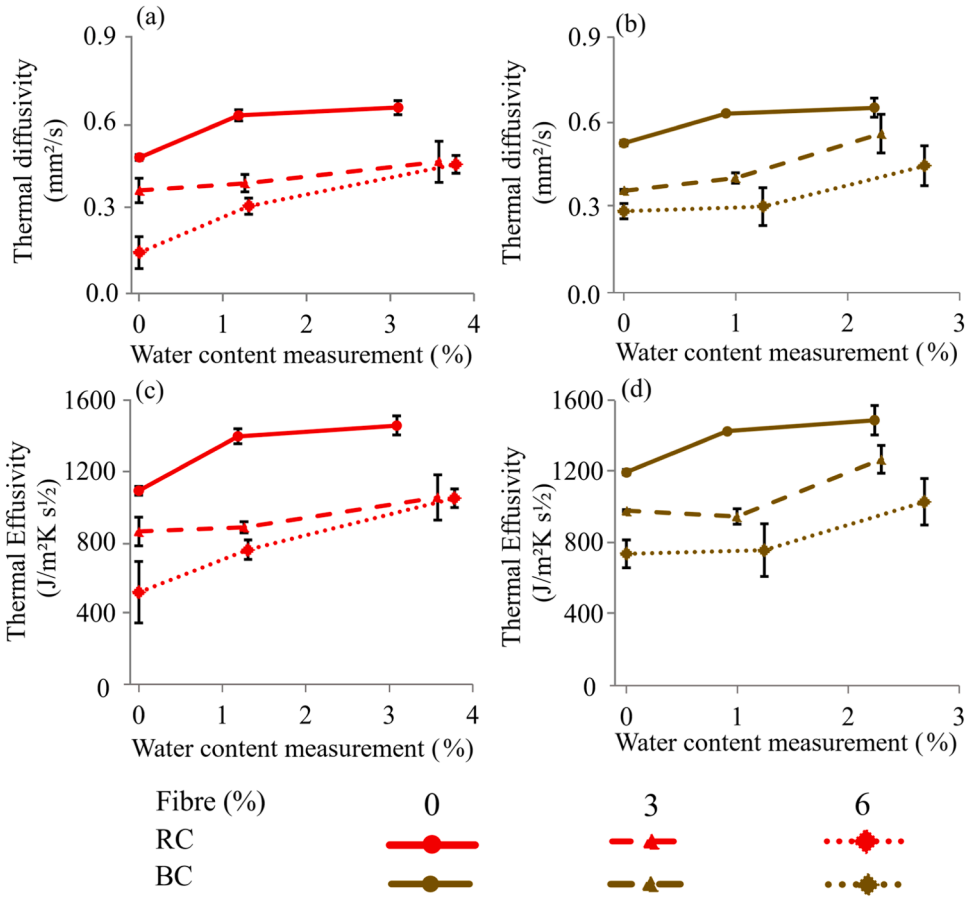

Fig. 8. Variation of diffusivity and thermal effusivity with water content of (a, c) red clay samples and (b, d) beige clay samples (b, d).

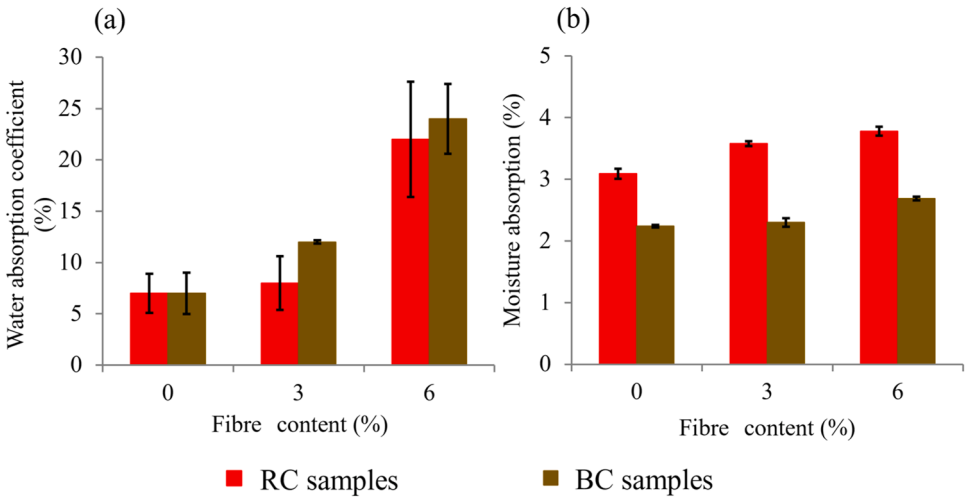

Fig. 9. Water and moisture absorption at a temperature of 23 ℃, (a) exposure to water for 24 hours and (b) exposure to 75 % RH for 48 hours.

samples resulted in a 47 % reduction in MBV value, while beige clay samples only led to a 5 % reduction. This is due to the influence of the fibres on the water vapor permeability and density of the samples. These coefficients are two major factors of the MBV value of the building materials.

3.4.4. *Sorption/desorption isotherms*

Fig. 12 shows the sorption/desorption curves determined for the 0 % wt, 3 %wt, and 6 %wt fibre samples and Table 4 shows the hydric properties determined according to the equations in Section 2.6. These properties represent the ability of materials to absorb and release moisture when a change in relative humidity occurs in their environment. The observed difference in Fig. 12d can be attributed to the use of shorter fibres in the fabrication of the beige clay samples containing 3 % fibres, compared to the first samples tested (results in Figs. 12a, 12b, 12c, 12e, and 12f). This modification results in a more pronounced hysteresis phenomenon than in the other absorption/desorption curves. This phenomenon is often related to the geometry of the pores, where

Table 3
Average value of water vapor permeability and water vapor resistance.

		Dry condition		Wet condition	
	Fibre (% wt)	δ x 10^{-11} (kg/s·m·Pa)	μ	δ x 10^{-11} (kg/s·m·Pa)	μ
RC	0	1.53 ± 0.05	14.52 ± 0.59	6.41 ± 0.20	3.57 ± 0.04
	3	1.40 ± 0.05	15.11 ± 0.39	4.57 ± 0.01	4.64 ± 0.17
	6	1.65 ± 0.05	14.71 ± 0.38	4.55 ± 0.90	5.32 ± 1.20
BC	0	1.18 ± 0.08	20.00 ± 1.35	4.75 ± 0.20	4.95 ± 0.11
	3	1.53 ± 0.20	16.08 ± 2.48	3.32 ± 0.19	7.40 ± 0.39
	6	1.27 ± 0.12	17.67 ± 0.91	3.53 ± 1.15	7.37 ± 3.36

the voids are interconnected by narrower passages, due to the short length of the fibres used in the formulation of these samples. The theoretical moisture buffer values (MBV_{Theor}), moisture effusivity (bm), moisture diffusivity (D_w), and equivalent moisture penetration depth ($dp_{1\,\%}$) values were calculated considering the moisture capacity (ξ) between 33 % and 75 %RH.

All red clay samples have higher experimental and theoretical MBV values than beige ones. The experimental MBV values are significantly higher than the theoretical MBV values obtained. The ANOVA test also showed a significant difference between the experimental and theoretical data (n = 6, α = 0.05, p-value = 0.001, Table S4, for supplementary information). This can be explained by the fact that ideal experimental conditions are rarely met, and film resistance due to the limited air layer on the sample exchange surface can affect measurement results [80]. The buffering capacity of construction materials helps to moderate indoor humidity fluctuations and reduce relative humidity peaks inside buildings [10,28,81]. Research has shown that the moisture buffering value is affected by the thickness of materials [82]. Understanding moisture buffering in materials is important for building design and energy efficiency considerations. The moisture diffusivity (D_w) and moisture effusivity (bm) decrease with the fibre content, in contrast to the specific moisture capacity (ξ), which increases with increasing fibres in the mixture.

The equivalent moisture penetration depth ($d_{p1\,\%}$) represents the minimum thickness that allows an uncoated wall to easily benefit from the moisture buffering effect to regulate the inside humidity [83]. In the

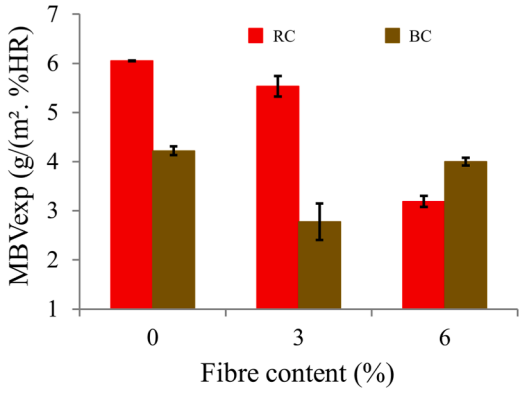

Fig. 11. MBV moisture buffer value of cob and clay materials.

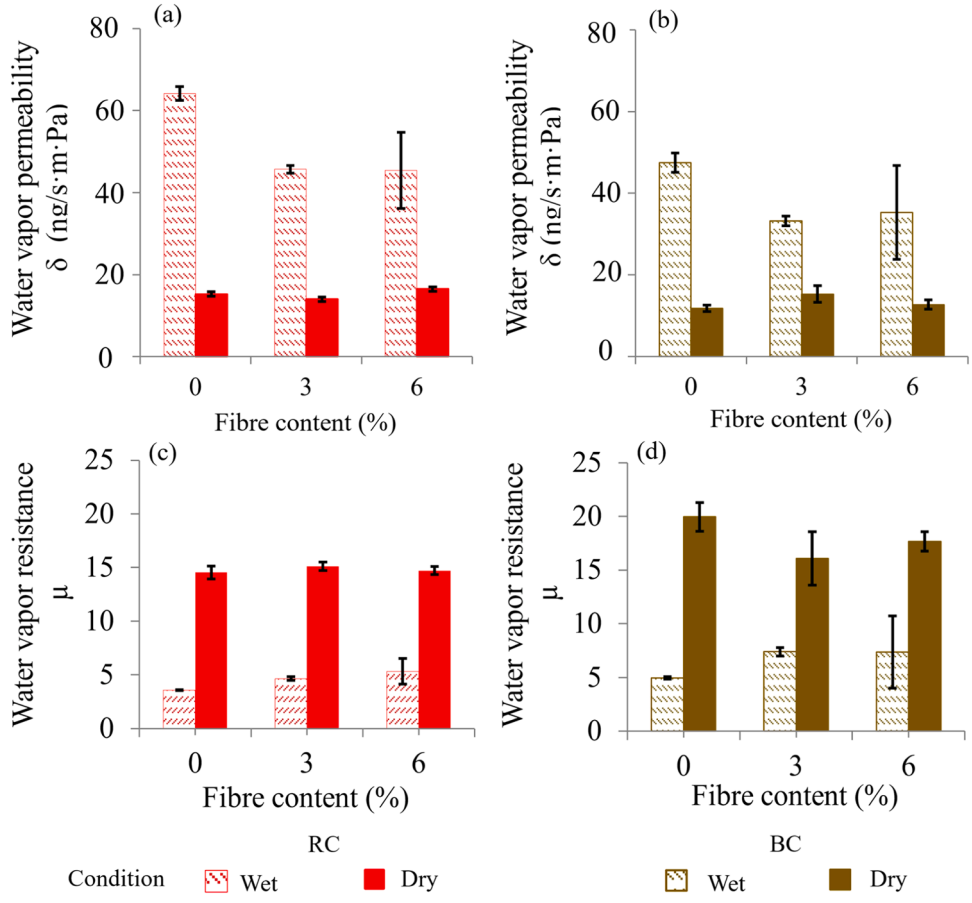

Fig. 10. Average values of water vapor permeability and water vapor resistance of (a and c) red and (b and d) beige clay samples.

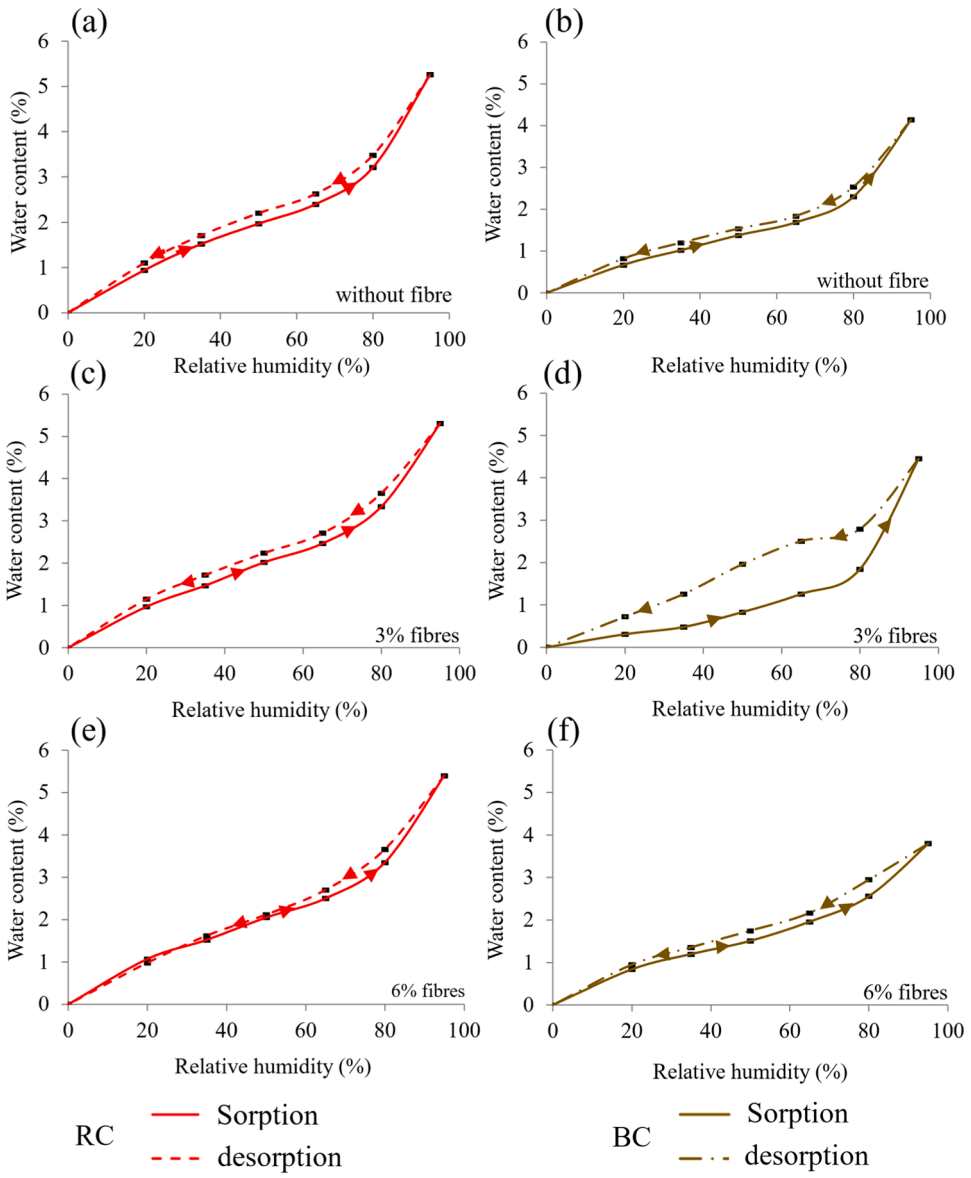

Fig. 12. Sorption/desorption curves for (a, c, and e) red and (b, d and f) beige clay samples.

Table 4
Calculated hydric properties and experimental for MBV_{exp}.

	Fibre (%wt)	ζ (kg/kg)	b_m (kg/m^2. Pa. s½)	D_w (m^2/s)	$d_{p1\ \%}$ (cm)	MBV_{Theor} (g/m^2.%HR)	MBV_{exp} (g/m^2.%HR)
RC	0	0.198	9.57×10^{-07}	4.49×10^{-09}	2.27	4.47	6.05
		± 0.0006	± 4.79×10^{-08}	± 7.63×10^{-10}	± 0.12	± 0.17	± 0.01
	3	0.0277	8.64×10^{-07}	2.80×10^{-09}	2.24	4.04	5.53
		± 0.0054	± 8.69×10^{-08}	± 4.75×10^{-10}	± 0.05	± 0.05	± 0.21
	6	0.0306	8.37×10^{-07}	2.95×10^{-09}	2.17	3.91	3.19
		± 0.0010	± 9.83×10^{-08}	± 5.19×10^{-10}	± 0.18	± 0.34	± 0.11
BC	0	0.0145	6.93×10^{-07}	4.70×10^{-09}	2.47	3.24	4.22
		± 0.0005	± 3.86×10^{-08}	± 9.35×10^{-10}	± 0.14	± 0.19	± 0.09
	3	0.0232	6.61×10^{-07}	2.52×10^{-09}	2.68	3.09	3.02
		± 0.0019	± 3.52×10^{-08}	± 1.58×10^{-10}	± 0.10	± 0.17	± 0.63
	6	0.0242	6.47×10^{-07}	2.98×10^{-09}	2.29	2.78	4.00
		± 0.0010	± 1.06×10^{-07}	±7.49×10^{-10}	± 0.10	± 0.37	± 0.08

context of building materials, the degree of moisture penetration is an important factor to consider to prevent issues such as water damage, mold growth, and structural decay. Controlling the equivalent moisture penetration depth is crucial for maintaining the integrity and longevity of buildings [52,84]. However, the available information on this coefficient in the literature only pertains to earth plasters without fibre additives for earth-based materials, specifically, in a study cited as [85]. In that study, the effect of adding fibres to clay samples was evaluated, and it was found that such an addition did not influence the equivalent moisture penetration depth (dp1 %). Understanding the equivalent

moisture penetration depth is crucial for selecting an appropriate wall thickness that optimizes the moisture buffering capacity of clay-based construction materials and other similar materials [85].

Fig. 13 shows the influence of relative humidity on the hydric properties of the samples. The specific moisture capacity, MBV, and moisture effusivity values of the samples show an increase in the 50–95 %RH relative humidity range. However, within the same relative humidity range, the moisture diffusivity decreases. These observed trends align with previous research, indicating that an increase in fibre content in samples leads to a decrease in both moisture diffusivity and moisture effusivity [80,83,86,87].

Fig. 14 shows the evolution of the equilibrium water content as a function of relative humidity. The sorption and desorption processes were very fast for each humidity step. From 20 % to 95 %RH, it took 50 days to reach the end of the sorption test and less than 50 days to lose the relative humidity absorbed during the test. Equilibrium is reached when the variation in the mass of the test samples does not exceed 0.0005 % for each humidity level. The attainment of equilibrium moisture content over time for samples subjected to increasing and decreasing relative humidity demonstrates that the response of the samples to a change in relative humidity is quite rapid and that equilibrium moisture values stabilize within four to eight days. These samples are capable of releasing the absorbed moisture during the sorption tests in less than eight days for each 15 % reduction in relative humidity at each interval (Fig. 14). This shows that these samples can easily regulate indoor humidity. No mold was observed during the tests (Visual inspection at each humidity level), which indicates that cob materials can regulate moisture up to 95 %RH without damage. The test results show an increase in the moisture absorbed by the samples without fibres as compared to the samples made with fibres. Its increase may be due to the fact that the small pores, with a higher specific surface area per unit volume, are favorable for water absorption [88].

3.5. Cob and interactions with humidity

The correlation between the variation in thermal and hygroscopic performance of clay and cob samples is complex and closely linked to moisture content and the presence of fibres (Figs. 7 and 8). Samples with a higher fibre content (6 % wt) show an increased capacity to absorb moisture (Table 2), which increases thermal conductivity. This effect is due to the enlargement of pores created by the fibres, allowing water vapor to replace air. When samples are exposed to a relative humidity of 50 % and 75 %, their capacity to absorb water increases, significantly influencing their thermal properties.

The increase in thermal conductivity due to moisture temporarily improves heat transfer through the material. This can be beneficial for thermal comfort in winter, as it allows for better heat distribution. However, this same characteristic can lead to excessive heat loss in winter and overheating in summer, thus reducing the overall energy efficiency of the building. Meanwhile, the specific heat of the samples also varies according to fibre and moisture content, with significant increases (Figs. 7c and 7d). A high thermal capacity allows the material

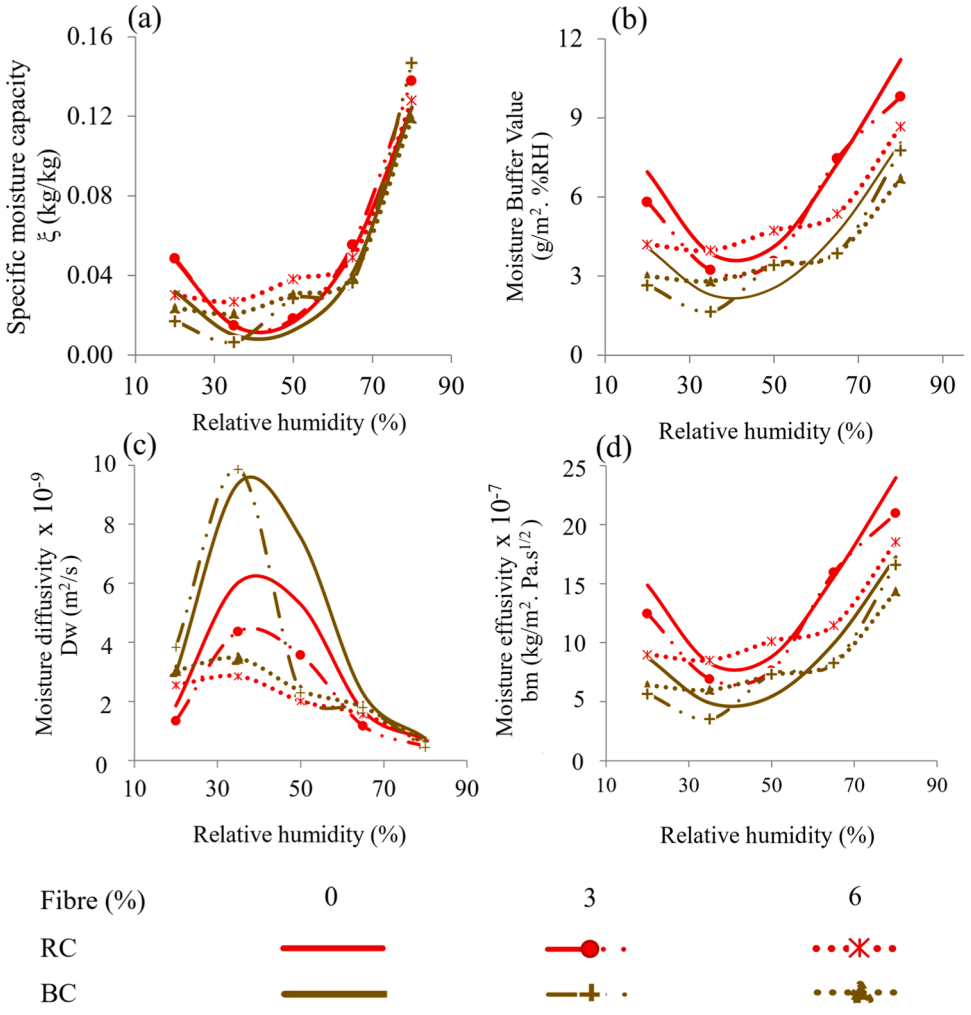

Fig. 13. Evolution of hydric properties with an increase in relative humidity: a) specific moisture capacity, b) moisture buffer value, c) moisture diffusivity, and d) moisture effusivity.

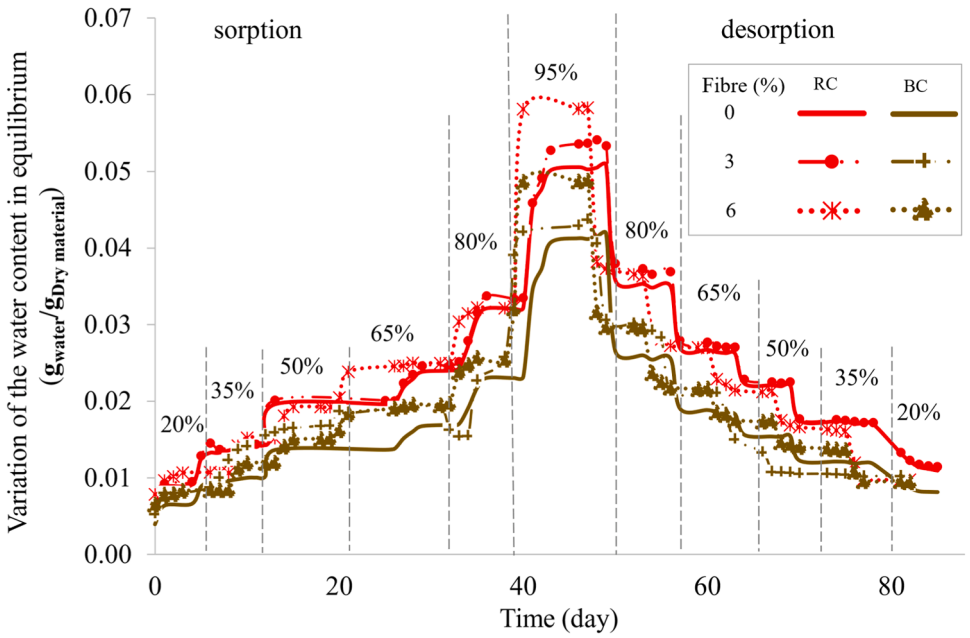

Fig. 14. Variation of the water content at equilibrium with increasing or decreasing relative humidity.

to store more heat, which can improve indoor thermal stability.

Regarding hygroscopic properties, the addition of fibres decreases water vapor permeability (Table 3) due to capillary retention in small pores, which increases resistance to vapor diffusion. Reduced permeability is beneficial for preventing excessive moisture penetration, but it can also limit the material's ability to breathe, which is crucial to avoid moisture accumulation and potential material degradation. The moisture buffer value (MBV) is also affected by fibre content. Red clay samples without fibres exhibit higher MBV values than reinforced ones (Fig. 11), which aligns with previous research showing that adding fibres can reduce MBV by increasing resistance to vapor diffusion. Overall, the correlation between thermal and hygroscopic performance of the samples is strongly influenced by fibre composition and water content, highlighting the importance of these factors in the design and

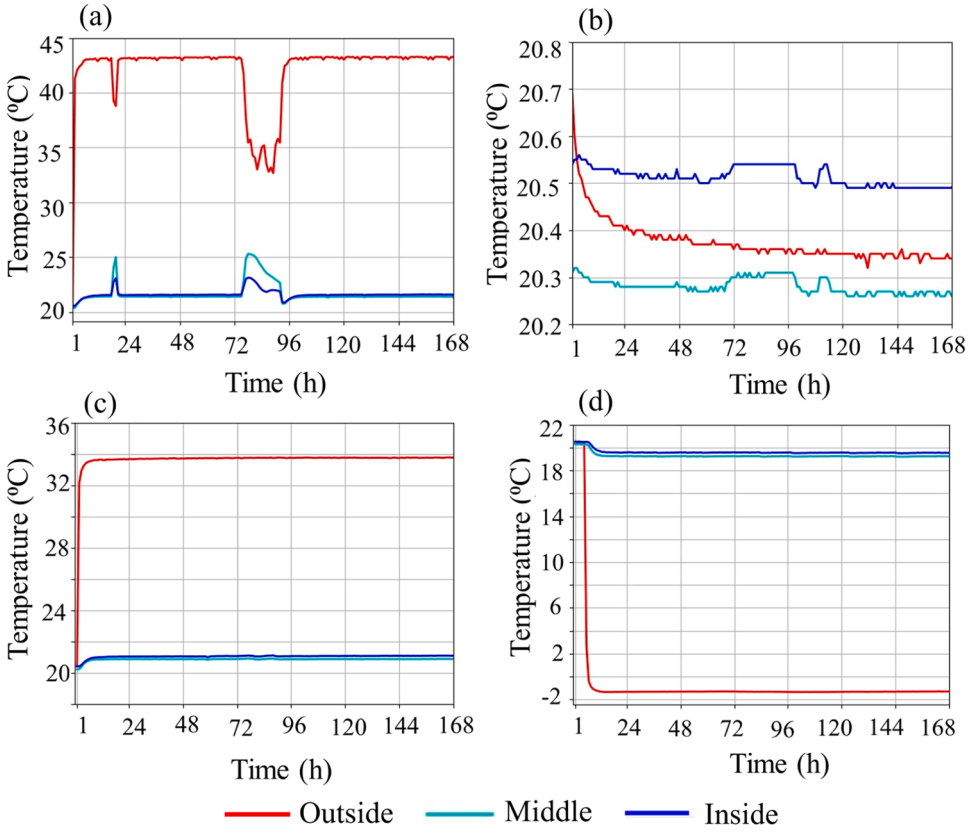

Fig. 15. Evolution of cob walls temperatures: a) dry season and b) cool season for City of Djibouti and c) dry season and d) cool season for City of Johannesburg.

optimization of clay and cob-based construction materials for optimal energy efficiency and moisture regulation.

3.6. Outside and inside temperatures in cob wall: experimental result

This section focuses on evaluating the temperature evolution of the outside, middle, and inside surfaces of a cob wall with 3 %wt fibres. The thermal and hydric properties of the wall material are detailed in Sections 3.3 and 3.4 of this article. Fig. 15 illustrates the temperature variation on the outside, middle, and inside surfaces of the cob wall during winter and summer. The external temperatures are set at 20 °C and −5 °C for Djibouti and Johannesburg, respectively in winter, and 45 °C and 35 °C for the same cities in summer. The measurements spanned 168 hours, which is equivalent to one week.

For the City of Djibouti, the outside wall surface temperature varied from 33 °C to 43 °C in the dry season (Fig. 15a), and between 20.3 °C and 20.4 °C in the cool season (Fig. 15b). On the inside wall surface, temperature varied between 21 °C and 23 °C. The maximum temperature of 23 °C was recorded at 8 p.m. on the first and third days of measurement before decreasing again (Fig. 15a). These phenomena were also observed for the middle wall temperatures when the exterior surface temperature of the wall dropped sharply to 33 °C and 39 °C (Fig. 15a). This phenomenon occurred due to a drop in the exterior environment temperature, set at 45 °C, caused by an air leakage issue, leading to a significant decrease in the exterior surface temperature of the wall during this period. For the City of Johannesburg, the outside wall surface temperature varied between 33.7 °C and 34 °C during the dry season (Fig. 15c) and between −1.4 °C and −1.3 °C during the cool season (Fig. 15d), an almost invisible, practically negligible variation. A slight temperature fluctuation was also observed on the inside surface of the wall during the dry season (from 21 °C to 21.1 °C) and during the cool season (from 19.5 °C to 19.6 °C), compared to the outside temperature set at 35 °C during the dry season and −5 °C during the cool season (Figs. 15c and 15d).

In the middle of the wall, the temperature variation was almost negligible, indicating that the heat transfer through the wall was very slow, except for the temperature drop observed in Fig. 15a. Fire resistance studies of composite earth materials have shown their ability to withstand fire and slow down heat penetration toward the unexposed face [89–92]. In-situ tests for cold climates have also provided reliable results for clay brick walls reinforced with plant fibres [90]. This can explain the low heat transfer towards the interior or the middle of the wall in our study.

These results show that a 15 cm thick cob wall exposed to low temperatures of −5 °C or high temperatures of +45 °C can maintain an inside temperature range of 19.5–23 °C for one week. The cob materials manufactured for laboratory tests may be suitable for construction sites due to their ease of large-scale production. Furthermore, the test walls have demonstrated good consistency between the wooden support and the cob materials made in the laboratory in terms of adhesion and non-detachment of the wooden supports and the material.

4. Conclusion

This study presents a series of experimental analyses of thermal properties as a function of moisture content and hygroscopic behavior of samples with different relative humidity. The fibres were wetted before being used to make the samples. Clay mixture samples with 3 %wt and 6 %wt fibre yielded interesting hygrothermal properties thanks to their ability to regulate high relative humidity without the risk of mold due to the presence of fibre. The effect of relative humidity on hygrothermal properties can therefore be summarized as follows.

- The thermal conductivity, specific heat, thermal diffusivity, and thermal effusivity increase with increasing water content. This phenomenon is attributable to the fact that the pores of the samples filled with air in the dry state are replaced by water vapor when exposed to increasing relative humidity.
- The moisture content of the samples reaches equilibrium around 4–8 days after the change in relative humidity, showing that the fibre-reinforced and fibre-free samples regulate the relative humidity well. Sorption tests showed that samples with 3 % and 6 % fibre can be exposed to very high relative humidity (80–95 %) for more than two weeks without risk of mold after a visual inspection.
- The samples studied exhibit an excellent moisture buffer value greater than 2 g/(m^2. %RH). This coefficient decreases for relative humidity between 20 % and 50 %RH and increases in relative humidity between 50 % and 95 %RH. The same trend was observed for the coefficients of specific moisture capacity and moisture effusivity, except that moisture diffusivity decreases with increasing relative humidity.
- Analysis of variance (ANOVA) and t-tests were used to demonstrate that the two clays have different hygrothermal behaviors. Also, the fibre content was confirmed to have a significant effect on hydric properties. However, the addition of fibres did not have an impact on the water vapor resistance factor (μ) and equivalent moisture penetration depth ($dp_{1\ \%}$) of all samples. The influence of surface film resistance on water vapor permeability was not considered in this study and is currently under investigation in our future work.
- The findings of the study on the 15 cm thick cob wall demonstrated its ability of cob to maintain a comfortable indoor temperature range of 19.5–23 °C for one week, even when exposed to extreme temperatures of −5 °C and +45 °C. These composite materials are suitable for constructing walls with a 15 cm or greater thickness. Their excellent thermal and moisture inertia make them an ideal choice for filling timber-frame structures, offering an effective solution for sustainable and eco-friendly construction. Furthermore, these materials are cost-effective and have the potential to significantly reduce energy consumption in buildings, resulting in affordable, low-carbon footprint, and healthy structures.

The water vapor permeability determined for all samples in this study is the apparent water vapor permeability, thus it does not consider the influence of surface film resistance. It would therefore be necessary to evaluate the actual water vapor permeability of cob materials and their evolution depending on the water content to observe their reaction to external humidity and its influence on moisture buffer values. All the results presented in this article pertain to the cob formulated with wheat fibres. Therefore, it is necessary to conduct a comprehensive evaluation of cob made with other plant fibres, using the same formulation techniques, in order to expand their use in the construction field.

CRediT authorship contribution statement

Claudiane Ouellet-Plamondon: Writing – review & editing, Validation, Supervision, Resources, Project administration, Methodology, Funding acquisition, Formal analysis, Data curation, Conceptualization. **Aguerata Kaboré:** Writing – original draft, Visualization, Validation, Methodology, Investigation, Data curation, Conceptualization. **Aziz Laghdir:** Writing – review & editing, Methodology, Formal analysis, Data curation.

Declaration of Competing Interest

The authors declare that they have no known competing financial interests or personal relationships that could have appeared to influence the work reported in this article.

Acknowledgments

This work was financed by the Pôle de Recherche et d'Innovation en Matériaux avancés du Québec (PRIMA), NSERC-Alliance (CRSNG

ALLRP 560404–20) and Mitacs (IT35572). It was also supported by the partners American Structures, Boralife, the Quebec Wood Export Bureau (QWEB), and ENERGIES 2050. The authors also thank SEREX for its participation in the hygrothermal properties measurements of the materials studied for this project and Patrick Brisebois, Ph.D., Chemistry, for reviewing and editing.

Appendix A. Supporting information

Supplementary data associated with this article can be found in the online version at doi:10.1016/j.conbuildmat.2024.138832.

Data availability

Data will be made available on request.

References

[1] J. Falana, R. Osei-Kyei, V.W. Tam, Towards achieving a net zero carbon building: A review of key stakeholders and their roles in net zero carbon building whole life cycle, J. Build. Eng. (2024) 108223, https://doi.org/10.1016/j.jobe.2023.108223.
[2] L. Wambersie, C. Ouellet-Plamondon, Developing a comprehensive account of embodied emissions within the Canadian construction sector, J. Ind. Ecol. (2024), https://doi.org/10.1111/jiec.13548.
[3] N.N. Myint, M. Shafique, Embodied carbon emissions of buildings: Taking a step towards net zero buildings, Case Stud. Constr. Mater. 20 (2024) e03024, https://doi.org/10.1016/j.cscm.2024.e03024.
[4] C. Ouellet-Plamondon, A. Kabore, Hygrothermal Measurement of Heavy Cob Materials, Springer Nature Switzerland, Cham, 2023, https://doi.org/10.1007/978-3-031-33211-1_111.
[5] A. Kaboré, C. Ouellet-Plamondon, Characterization of the clay and fibres for hygrothermal modelling. Canadian Society of Civil Engineering Annual Conference, Springer, 2021, https://doi.org/10.1007/978-981-19-1004-3_29.
[6] M. Moudjari, et al., Using Local Mater. Optim. eco-Des. a resilient Urban Environ. Sustain. Urban Proj. Process (2021), https://doi.org/10.13189/cea.2021.090636.
[7] F. Pacheco-Torgal, S. Jalali, Earth construction: lessons from the past for future eco-efficient construction, Constr. Build. Mater. 29 (2012) 512–519, https://doi.org/10.1016/j.conbuildmat.2011.10.054.
[8] S. Goodhew, et al., Improving the thermal performance of earthen walls to satisfy current building regulations, Energy Build. 240 (2021) 110873, https://doi.org/10.1016/j.enbuild.2021.110873.
[9] S. Liuzzi, et al., Hygrothermal properties of clayey plasters with olive fibers, Constr. Build. Mater. 158 (2018) 24–32, https://doi.org/10.1016/j.conbuildmat.2017.10.013.
[10] A. Laborel-Préneron, C. Magniont, J.-E. Aubert, Hygrothermal properties of unfired earth bricks: Effect of barley straw, hemp shiv and corn cob addition, Energy Build. 178 (2018) 265–278, https://doi.org/10.1016/j.enbuild.2018.08.021.
[11] M. Bouasria, et al., Valorisation of stranded Laminaria digitata seaweed as an insulating earth material, Constr. Build. Mater. 308 (2021) 125068, https://doi.org/10.1016/j.conbuildmat.2021.125068.
[12] S. Dubois, et al., An inverse modelling approach to estimate the hygric parameters of clay-based masonry during a Moisture Buffer Value test, Build. Environ. 81 (2014) 192–203, https://doi.org/10.1016/j.buildenv.2014.06.018.
[13] F. McGregor, et al., Conditions affecting the moisture buffering measurement performed on compressed earth blocks, Build. Environ. 75 (2014) 11–18, https://doi.org/10.1016/j.buildenv.2014.01.009.
[14] F. McGregor, et al., The moisture buffering capacity of unfired clay masonry, Build. Environ. 82 (2014) 599–607, https://doi.org/10.1016/j.buildenv.2014.09.027.
[15] F. McGregor, et al., A review on the buffering capacity of earth building materials, Proc. Inst. Civ. Eng. -Constr. Mater. 169 (5) (2016) 241–251, https://doi.org/10.1680/jcoma.15.00035.
[16] K.A.J. Ouedraogo, et al., Is stabilization of earth bricks using low cement or lime contents relevant? Constr. Build. Mater. 236 (2020) 117578 https://doi.org/10.1016/j.conbuildmat.2019.117578.
[17] C. Chabaud, Les filières lin et chanvre au cœur des enjeux des matériaux biosourcés émergents, J. Off. De. la R. éPublique Française 16 (2015).
[18] D. Hammiche, et al., Etude des Propriétés Physico-chimiques, Thermiques et Mécaniques des Fibres d'Alfa Grasses. Revue des Composites et des Matériaux avancés, J. Compost. Adv. Mat. 25 (2015) 7–24.
[19] I. Akinwumi, earth Build. Constr. Process. Benin City, Niger. Eng. Classif. earth Mater. Use (2014).
[20] E. Hamard, et al., Cob, a vernacular earth construction process in the context of modern sustainable building, Build. Environ. 106 (2016) 103–119, https://doi.org/10.1016/j.buildenv.2016.06.009.
[21] Al Haffar, N., et al. *Cement stabilization effect on mechanical and hygric properties of compacted earth*. in Fifth International Conference on Sustainable Construction Materials and Technologies. ⟨http://www.claisse.info/Proceedings.htm⟩. 2019.
[22] N. Jannat, et al., Application of agro and non-agro waste materials for unfired earth blocks construction: a review, Constr. Build. Mater. 254 (2020) 119346, https://doi.org/10.1016/j.conbuildmat.2020.119346.
[23] B. Taallah, et al., Mechanical properties and hygroscopicity behavior of compressed earth block filled by date palm fibers, Constr. Build. Mater. 59 (2014) 161–168, https://doi.org/10.1016/j.conbuildmat.2014.02.058.
[24] G. Di Bella, et al., Effects of natural fibres reinforcement in lime plasters (kenaf and sisal vs. Polypropylene), Constr. Build. Mater. 58 (2014) 159–165, https://doi.org/10.1016/j.conbuildmat.2014.02.026.
[25] M. Labat, et al., From the experimental characterization of the hygrothermal properties of straw-clay mixtures to the numerical assessment of their buffering potential, Build. Environ. 97 (2016) 69–81, https://doi.org/10.1016/j.buildenv.2015.12.004.
[26] N.S.N. Arman, R.S. Chen, S. Ahmad, Review of state-of-the-art studies on the water absorption capacity of agricultural fiber-reinforced polymer composites for sustainable construction, Constr. Build. Mater. 302 (2021) 124174, https://doi.org/10.1016/j.conbuildmat.2021.124174.
[27] R. Bui, M. Labat, J.-E. Aubert, Comparison of the Saturated Salt Solution and the Dynamic Vapor Sorption techniques based on the measured sorption isotherm of barley straw, Constr. Build. Mater. 141 (2017) 140–151, https://doi.org/10.1016/j.conbuildmat.2017.03.005.
[28] B.K. Kreiger, W.V. Srubar, III, Moisture buffering in buildings: a review of experimental and numerical methods, Energy Build. 202 (2019) 109394, https://doi.org/10.1016/j.enbuild.2019.109394.
[29] Cf.A.H.Fi.A. CAHF, Finacment du Logement En. Afr.: Exam. Des. marchéS. De. Financ. De. Certains pays D. 'Afr. (2017) 290.
[30] M. Majale, G. Tipple, M. French, Affordable land and housing in Africa, U. Nations Hum. Settl. Program. 3 (2011) 101. ⟨http://www.unhabitat.org⟩.
[31] O. Yetunde, Multi–habitation: a form of Housing in African Urban Environments, IOSR J. Environ. Sci., Toxicol. Food Technol. 8 (4) (2014) 06. ⟨www.iosrjournals.org⟩.
[32] E.-H.M. Bah, I. Faye, Z. Geh, Springer Nature, Hous. Mark. Dyn. Afr. (2018).
[33] V. Zoma, N. Nakanabo, L'habitat informel en Afrique, GRIN Verlag, 2022. ⟨https://hal.science/hal-03955100⟩.
[34] E. Meyer, Temp. Stab. Tradit. Low. -Cost. Mod. Hous. East. Cape, South Afr. (2010) 13.
[35] R. Tomovska, A. Radivojević, Tracing sustainable design strategies in the example of the traditional Ohrid house, J. Clean. Prod. 147 (2017) 10–24, https://doi.org/10.1016/j.jclepro.2017.01.073.
[36] A. Azil, et al., Earth construction: Field variabilities and laboratory reproducibility, Constr. Build. Mater. 314 (2022) 125591, https://doi.org/10.1016/j.conbuildmat.2021.125591.
[37] K. Haddad, S. Lannon, E. Latif, Investigation of Cob construction: Review of mix designs, structural characteristics, and hygrothermal behaviour, J. Build. Eng. (2024) 108959, https://doi.org/10.1016/j.jobe.2024.108959.
[38] M. Gomaa, et al., Thermal performance exploration of 3D printed cob, Archit. Sci. Rev. 62 (3) (2019) 230–237, https://doi.org/10.1080/00038628.2019.1606776.
[39] A.M. Kabore, Ouellet-Plamondon, Improved insulation with fibres in heavy cob for building walls, Ind. Crops Prod. 215 (2024) 118626, https://doi.org/10.1016/j.indcrop.2024.118626.
[40] A. Kabore, C.M. Ouellet-Plamondon, The impact of vegetable fibres on the shrinkage and mechanical properties of cob materials, Materials 17 (3) (2024) 736, https://doi.org/10.3390/ma17030736.
[41] S.H. Sameh, Promoting earth architecture as a sustainable construction technique in Egypt, J. Clean. Prod. 65 (2014) 362–373, https://doi.org/10.1016/j.jclepro.2013.08.046.
[42] A. Gounni, H. Louahlia, Dynamic behavior and economic analysis of sustainable building integrating cob and phase change materials, Constr. Build. Mater. 262 (2020) 120795, https://doi.org/10.1016/j.conbuildmat.2020.120795.
[43] CAN/BNQ-2501-090, Sols - Determination de la limite de liquidite a l'aide de l'appareil de Casagrande et de la limite de plasticite, Stand. Counc. Can. (2011).
[44] M. Aouinti, Sorption du produit de traitement de bois par l'argile dans la construction en terre: cas de l'octaborate disodique tétrahydraté (DOT), École de technologie supérieure, 2023. ⟨https://espace.etsmtl.ca/id/eprint/3181⟩.
[45] I.I. Ikelle, O.S.P. Ivoms, Determination of the heating ability of coal and corn cob briquettes, IOSR J. Appl. Chem. 7 (2) (2014) 77–82.
[46] ASTM D2654-89a, Standard Test Method for Moisture in Textile. ASTM D2654–89a, ASTM, *West Conshohocken, PA, USA*, 1989, p. 10. ⟨https://global.ihs.com/doc_detail.cfm?document_name=ASTM%20D2654&item_s_key=00016807⟩.
[47] T.N. Ho Thi, Étude de l'influence de la température et de l'humidité sur les propriétés mécaniques en traction des fibres de chanvre et de coco, École de technologie supérieure, 2008. ⟨https://espace.etsmtl.ca/id/eprint/128⟩.
[48] NF ISO 5017, Dense-shaped refractory products - Determination of bulk density, apparent porosity and true porosity, NF ISO 5017. 2013. ⟨https://sagaweb.afnor.org/fr-FR/sw/Consultation/Notice/1400375?directFromSearch=true⟩.
[49] ASTM D7984, Méthode d'essai standard pour la mesure de l'effusivité thermique des tissus à l'aide d'un instrument à source plane transitoire modifiée (MTPS), ASTM International, 2016.
[50] ISO 15148, Hygrothermal performance of building materials and products — Determination of water absorption coefficient by partial immersion 2002: p. 11p. ⟨https://standards.iteh.ai/catalog/standards/sist/5ab182e2-a7ad-428c-87e1-40fe97b42300/iso-15148-2002⟩.
[51] ASTME96-95, Standard test methods for water vapor transmission of materials, ASTM committe on Standards, 100 Barr Harbor Drive, West Coshohocken, PA 19428-2959, United States, 1995. ⟨https://compass.astm.org/document/?contentCode=ASTM%7CE0096_E0096M-16%7Cen-US⟩.
[52] C. Rode, et al., Moisture buffering of building materials, Technical University of Denmark, Department of Civil Engineering, 2005. ⟨https://vbn.aau.dk/ws/files/235442745/byg-r126.pdf⟩.

[53] ISO 12571, 12571–Performance hygrothermique des matériaux et produits pour le bâtiment–Détermination des propriétés de sorption hygroscopique. 22p Troisieme edition: Octobre., 2021.
[54] M. Sawadogo, et al., Development and hygrothermal performance analysis of a novel eco-friendly insulating wall under various climatic conditions, Build. Environ. 245 (2023) 110841, https://doi.org/10.1016/j.buildenv.2023.110841.
[55] Openweather, Current & Forecast weather data collection. s.d. ⟨https://openweathermap.org/api⟩.
[56] M. Bouasker, et al., Physical characterization of natural straw fibers as aggregates for construction materials applications, Materials 7 (4) (2014) 3034–3048, https://doi.org/10.3390/ma7043034.
[57] M. Dallel, Evaluation du potentiel textile des fibres d'Alfa (Stipa Tenacissima L.): Caractérisation physico-chimique de la fibre au fil, Université de Haute Alsace-Mulhouse, 2012. ⟨https://theses.hal.science/tel-00844129/⟩.
[58] A.D.O. Betené, et al., Influence of sampling area and extraction method on the thermal, physical and mechanical properties of Cameroonian Ananas comosus leaf fibers, Heliyon 8 (8) (2022) e10127. ⟨https://www.cell.com/heliyon/pdf/S2405-8440(22)01415-3.pdf⟩.
[59] S. Hamza, et al., Physico-chemical characterization of Tunisian plant fibers and its utilization as reinforcement for plaster based composites, Ind. Crops Prod. 49 (2013) 357–365, https://doi.org/10.1016/j.indcrop.2013.04.052.
[60] S. Liuzzi, C. Rubino, P. Stefanizzi, Use of clay and olive pruning waste for building materials with high hygrothermal performances, Energy Procedia 126 (2017) 234–241, https://doi.org/10.1016/j.egypro.2017.08.145.
[61] L. Randazzo, et al., Moisture absorption, thermal conductivity and noise mitigation of clay based plasters: the influence of mineralogical and textural characteristics, Appl. Clay Sci. 132 (2016) 498–507, https://doi.org/10.1016/j.clay.2016.07.021.
[62] F. Alassaad, et al., Improvement of cob thermal inertia by latent heat storage and its implication on energy consumption, Constr. Build. Mater. 329 (2022) 127163, https://doi.org/10.1016/j.conbuildmat.2022.127163.
[63] M.B. Mansour, et al., Optimizing thermal and mechanical performance of compressed earth blocks (CEB), Constr. Build. Mater. 104 (2016) 44–51, https://doi.org/10.1016/j.conbuildmat.2015.12.024.
[64] T.A. Phung, Formulation et caractérisation d'un composite terre-fibres végétales: la bauge, Normandie Université, 2018. ⟨https://theses.hal.science/tel-01938827⟩.
[65] A. Azil, et al., Monitoring of drying kinetics evolution and hygrothermal properties of new earth-based materials using climatic chamber simulation, Case Stud. Constr. Mater. 18 (2023) e01798, https://doi.org/10.1016/j.cscm.2022.e01798.
[66] R. Sadouri, H. Kebir, M. Benyoucef, The effect of incorporating alfa fibers on the properties of compressed stabilized earth blocks, Eur. -Mediterr. J. Environ. Integr. (2024) 1–15, https://doi.org/10.1007/s41207-024-00561-9.
[67] T.A. Phung, et al., Hygrothermal behaviour of cob material. Earthen Dwellings and Structures, Springer, 2019, pp. 345–356, https://doi.org/10.1007/978-981-13-5883-8_30.
[68] A.-M. Tang, Y.-J. Cui, T.-T. Le, A study on the thermal conductivity of compacted bentonites, Appl. Clay Sci. 41 (3-4) (2008) 181–189, https://doi.org/10.1016/j.clay.2007.11.001.
[69] E. Anglade, et al., Physical and mechanical properties of clay–sand mixes to assess the performance of earth construction materials, J. Build. Eng. 51 (2022) 104229, https://doi.org/10.1016/j.jobe.2022.104229.
[70] M.S. Abbas, et al., Effect of moisture content on hygrothermal properties: comparison between pith and hemp shiv composites and other construction materials, Constr. Build. Mater. 340 (2022) 127731, https://doi.org/10.1016/j.conbuildmat.2022.127731.
[71] A. Mellaikhafi, et al., Characterization and thermal performance assessment of earthen adobes and walls additive with different date palm fibers, Case Stud. Constr. Mater. 15 (2021) e00693, https://doi.org/10.1016/j.cscm.2021.e00693.
[72] F. Alassaad, et al., Effect of latent heat storage on thermal comfort and energy consumption in lightweight earth-based housings, Build. Environ. 229 (2023) 109915, https://doi.org/10.1016/j.buildenv.2022.109915.
[73] D. Khoudja, et al., Mechanical and thermophysical properties of raw earth bricks incorporating date palm waste, Constr. Build. Mater. 270 (2021) 121824, https://doi.org/10.1016/j.conbuildmat.2020.121824.
[74] A. Laborel-Préneron, et al., Plant aggregates and fibers in earth construction materials: a review, Constr. Build. Mater. 111 (2016) 719–734, https://doi.org/10.1016/j.conbuildmat.2016.02.119.
[75] H. Cagnon, et al., Hygrothermal properties of earth bricks, Energy Build. 80 (2014) 208–217, https://doi.org/10.1016/j.enbuild.2014.05.024.
[76] F. Fouchal, et al., Experimental evaluation of hydric performances of masonry walls made of earth bricks, geopolymer and wooden frame, Build. Environ. 87 (2015) 234–243, https://doi.org/10.1016/j.buildenv.2015.01.036.
[77] M. O'Farrell, S. Wild, B. Sabir, Pore size distribution and compressive strength of waste clay brick mortar, Cem. Concr. Compos. 23 (1) (2001) 81–91, https://doi.org/10.1016/S0958-9465(00)00070-6.
[78] A.W. Bruno, D. Gallipoli, Hygro-mechanical characterisation of hypercompacted earth for building construction, Université de Pau et des Pays de l'Adour-Laboratoire SIAME, 2016. ⟨https://univ-pau.hal.science/tel-02366888⟩.
[79] M. Palumbo, et al., The influence of two crop by-products on the hygrothermal properties of earth plasters, Build. Environ. 105 (2016) 245–252, https://doi.org/10.1016/j.buildenv.2016.06.004.
[80] I. Gómez, et al., Moisture buffering performance of a new pozolanic ceramic material: influence of the film layer resistance, Energy Build. 43 (4) (2011) 873–878, https://doi.org/10.1016/j.enbuild.2010.12.007.
[81] M. Zhang, et al., Moisture buffering phenomenon and its impact on building energy consumption, Appl. Therm. Eng. 124 (2017) 337–345, https://doi.org/10.1016/j.applthermaleng.2017.05.173.
[82] S. Khaled, et al., Effect of air velocity and initial conditioning on the moisture buffer value of four different building materials, Materials 16 (8) (2023) 3284, https://doi.org/10.3390/ma16083284.
[83] F. Collet, S. Pretot, Experimental investigation of moisture buffering capacity of sprayed hemp concrete, Constr. Build. Mater. 36 (2012) 58–65, https://doi.org/10.1016/j.conbuildmat.2012.04.139.
[84] J. Woods, J. Winkler, D. Christensen, Evaluation of the effective moisture penetration depth model for estimating moisture buffering in buildings, National Renewable Energy Lab.(NREL), Golden, CO (United States), 2013, https://doi.org/10.2172/1067948.
[85] D. Maskell, et al., Determination of optimal plaster thickness for moisture buffering of indoor air, Build. Environ. 130 (2018) 143–150, https://doi.org/10.1016/j.buildenv.2017.11.045.
[86] M. Rahim, et al., Characterization of flax lime and hemp lime concretes: hygric properties and moisture buffer capacity, Energy Build. 88 (2015) 91–99, https://doi.org/10.1016/j.enbuild.2014.11.043.
[87] A.D.T. Le, Etude des transferts hygrothermiques dans le béton de chanvre et leur application au bâtiment (sous titre: simulation numérique et approche expérimentale), Université de Reims-Champagne Ardenne, 2010.
[88] L. Wang, et al., High-pressure hydrogen adsorption in clay minerals: Insights on natural hydrogen exploration, Fuel 344 (2023) 127919, https://doi.org/10.1016/j.fuel.2023.127919.
[89] L. Gonzalez-Lopez, et al., Study of the fire and thermal behaviour of façade panels made of natural fibre-reinforced cement-based composites, Constr. Build. Mater. 302 (2021) 124195, https://doi.org/10.1016/j.conbuildmat.2021.124195.
[90] R. Zhao, et al., Research on thermal insulation properties of plant fiber composite building material: a review, Int. J. Thermophys. 41 (2020) 1–18, https://doi.org/10.1007/s10765-020-02665-0.
[91] Q. Nguyen, et al., Fire performance of prefabricated modular units using organoclay/glass fibre reinforced polymer composite, Constr. Build. Mater. 129 (2016) 204–215, https://doi.org/10.1016/j.conbuildmat.2016.10.100.
[92] A.B. Alabi, et al., Cooling effect of some materials in clay composite bricks for tropical region, FUTY J. Environ. 8 (1) (2014) 1–7.